Digest Journal of Nanomaterials and Biostructures Vol. 19, No. 4, October-December 2024, p. 1383-1394

Effects of cadmium doping on the physical and sensing properties of nanostructured CuO thin films

H. R. Shakir[a], S. K. Dawood[b], K. N. Hussein[c], S. S. Chiad[d], F. A. Jasim[b] *, N. F. Habubi[e], Y. H. Kadhim[f] M. Jadan[g, h]

[a]*Department of Optometry, Technical Medical Institute - Al-Mansur, Middle Technical University, Iraq*
[b]*Department of Physics, College of Science, Mustansiriyah University, Iraq*
[c]*Department of Radiology, Al-Manara College for Medical Science, Iraq*
[d]*Department of Physics, College of Education, Mustansiriyah University, Iraq*
[e]*Department of Radiation and Sonar Technologies, Alnukhba University College, Iraq*
[f]*Department of Optics Techniques, College of Health and Medical Techniques, AL-Mustaqbal University, Babylon, Hillah, 51001, Iraq*
[g]*Department of Physics, College of Science, Imam Abdulrahman Bin Faisal University, P.O. Box 1982, 31441 Dammam, Saudi Arabia*
[h]*Basic and Applied Scientific Research Center, Imam Abdulrahman Bin Faisal University, P.O. Box 1982, 31441 Dammam, Saudi Arabia*

This investigation used sol-gel deposition to create undoped CuO and CuO: Cd thin films. All films of undoped CuO and CuO: Cd phase exhibit four dominating peaks at 35.52°, 38.84°, 53.37°, and 68.23°, which are correspondingly assigned to the (022), (200), (020), and (220) planes, according to X-ray diffraction analysis. The dislocation density reduced from 60.55 to 49.94, the strain decreased from 26.98 to 24.60, and the grain size of the produced films measured by XRD was 12.85–14.15 nm. Atomic force microscopy (AFM) was used to study the morphology. SEM analysis showed increased aggregation with higher Cd content, resulting in a more uniform porous structure. The optical band gap decreases for all samples as the cadmium content increases, ranging from 2.28 to 2.14 eV. Similarly, the refractive index and extinction coefficient values decrease as the cadmium content increases for all samples. The gas sensor detects H_2 (375 ppm) using CuO film cadmium doping, which enhances sensitivity, CuO: 4% exhibits highest resistance. Sensitivity decreases with higher doping, indicating reduced sensor responsiveness.

(Received May 18, 2024; Accepted September 18, 2024)

Keywords: CuO, Cd thin film, Sol-gel technique, Structural, morphological and optical properties, Band gap

1. Introduction

Researchers from all around the world are interested in the semiconducting metal oxide nanostructures. Numerous technological disciplines, including biotechnology, microelectronics, the solar industry, corrosion, etc., have used this material in diverse applications [1-3]. Most approaches nowadays are utilized to shrink materials to the nanoscale, which causes these materials to exhibit novel and distinctive characteristics in optical, electrical, optoelectronic, dielectric, and other fields [4, 5]. Examples of its numerous uses include lithium-ion electrodes, sensors, field emission, and photocatalysts [6,7]. CuO is a p-type semiconductor material [8, 9]. CuO thin films are produced using a variety of techniques, including the electrodeposition technique [10,11], CVD [12,13], reflux condensation [14], spray pyrolysis [15], SILAR [16], sol-gel [17], magnetron sputtering [18-20] and thermal oxidation [21].

* Corresponding author: Farah.A.J@uomustansiriyah.edu.iq
https://doi.org/10.15251/DJNB.2024.194.1383

In this study, we utilized the Sol-gel technique, known for its simplicity and compatibility with non-vacuum environments, to deposit films on various substrate types. The Sol-gel method was employed to prepare the CuO and CuO: Cd solutions utilized in this research, which were subsequently coated onto glass substrates. The primary objective of this paper was to investigate the impact of cadmium doping on the structural, morphological, and optical properties of CuO films.

2. Experimental

The undoped CuO and CuO:Cd thin films were fabricated using the sol-gel spin-coating method. To dissolve 0.2 M copper acetate monohydrate, 2-methoxyethanol [$CH_3OCH_2CH_2CH_2OH$] was utilized as the solvent. For doping with 1% and 3% Cadmium, Cadmium nitrate [$Cd(NO_3)_3.9H_2O$] was employed. Monoethanolamine [$OHCH_2CH_2NH_2$] was a stabilizer, maintaining a 1:1 mole ratio with the precursor, following steady magnetic stirring for 10 minutes at room temperature. The solution underwent 1-hour agitation at 70°C before being aged for 24 hours at room temperature. Before the deposition, bases were cleaned sequentially with acetone, ethanol, and deionized water to ensure uniformity. A two-step spinning technique was employed to achieve this. Initially, the solution was applied to the substrate at 100 rpm for 15 seconds, followed by a subsequent cycle at 3000 rpm for 20 seconds. After each of the four deposition cycles, the film was dried on a hotplate for 10 minutes at 160 °C. All thin films underwent an air-conditioned, one-hour annealing process at 500 °C. Then, XRD analysis examines samples' structural information (XRD: Model D8 advance Bruker). Additionally, samples' morphology is investigated utilizing AFM analysis. The AFM Fig. is tridimensional, and the scan zone is 2 by 2 meters. The surface morphology was investigated using a scanning electron microscope. Spectroscopy analysis to obtain the transmission spectrum using (UV-visible: scan of Model Gray 500). The CuO gas sensor was made using aluminum electrodes on thin films. Gas sensitivity was assessed by the percentage change in resistance within a cylindrical chamber (radius: 8 cm, height: 16 cm).

3. Results and discussions

XRD analysis is the primary technique to characterize the phases of the grown films. Fig. 1 depicts the XRD patterns regarding ICDD card No. (05-0661). In the Cd-doped CuO films, the Cd phase displays prominent peaks at 35.52°, 38.84°, 53.37°, and 68.23° corresponding to the (002), (200), (020), and (220) planes, respectively. Notably, the intensity of the (002) reflections increases with higher doping levels, indicating a shift towards the monoclinic phase with a strong preferred orientation [22, 23]. Additionally, the crystallite size (D), as determined by Scherrer's formula, shows an increase with the amount of cadmium incorporated [24, 25].

$$D = \frac{0.9\lambda}{\beta cos\theta} \quad (1)$$

The decrease in β (FWHM) of peaks with increasing cadmium concentration suggests a refinement in the crystalline structure of the thin films. This phenomenon can be attributed to incorporating cadmium atoms into the CuO lattice, which may improve crystallinity and reduce defects. The rise in average grain size from 12.47 to 14.15 nm with increasing cadmium concentration further supports the notion that cadmium has a significant impact on determining the size of material crystals. This increase in grain size indicates a more pronounced crystalline growth in the presence of higher cadmium levels, which can influence the overall properties and performance of the thin films [26-28].

The dislocation density (δ) can be calculated using the following formula [29, 30]:

$$\delta = \frac{1}{D^2} \quad (2)$$

Furthermore, Eq. 3 was employed to calculate the lattice strain (ε) [31]:.

$$\varepsilon = \frac{\beta cos\theta}{4} \quad (3)$$

It was observed that as the Cadmium doping increased, both the computed dislocation density values (δ) and strain (δ) exhibited a decreasing trend [29]. Each of FWHM, D, and lattice strain (ε) is depicted in Fig. (2) as a function of the Cadmium concentration. This graphical representation provides a visual understanding of how these parameters vary with increasing levels of Cadmium doping [32, 33].

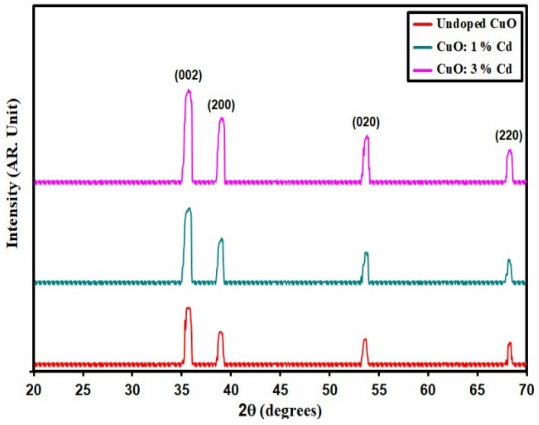

Fig. 1. XRD styles of grown films.

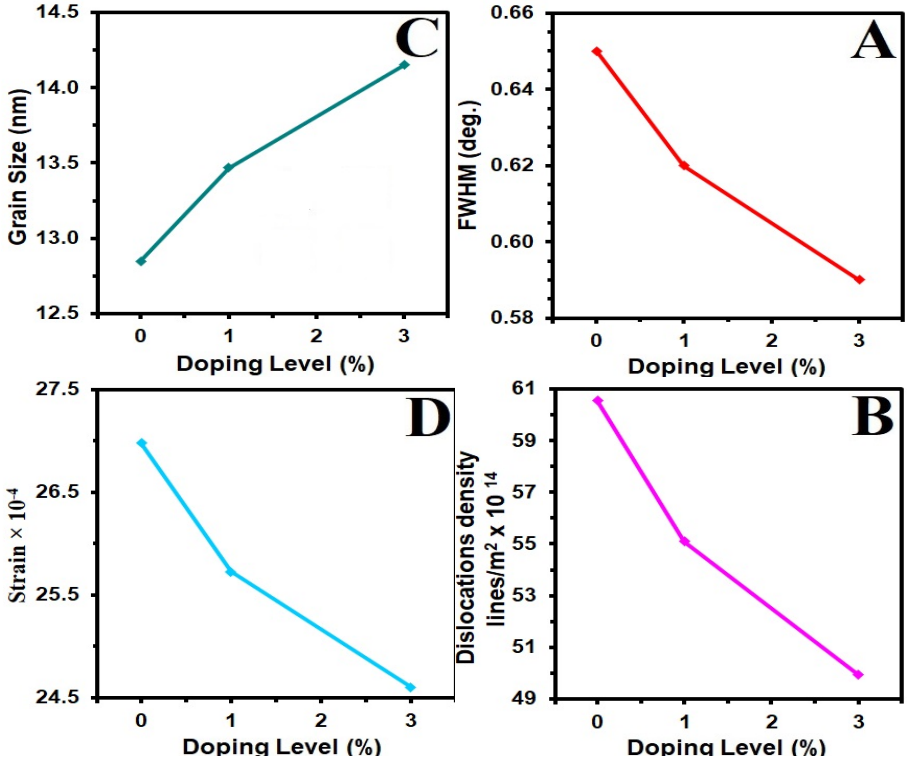

Fig. 2. FWHM (a) D (b) δ (c) ε (d) of the grown films

.

Table 1. D, E_g and structural coefficient of grown films.

Sample	2 θ (°)	(hkl) Plane	FWHM (°)	E_g (eV)	*D* (nm)	δ(× 10^{14}) (lines/m^2)	ε (× 10^{-4})
Undoped CuO	35.84	002	0.65	2.28	12.85	60.55	26.98
CuO: 1% Cd	35.80	002	0.62	2.20	13.47	55.10	25.73
CuO: 3% Cd	35.77	002	0.59	2.14	14.15	49.94	24.60

Fig. 3 presents the surface morphology of undoped CuO and CuO films doped with 2% and 4% Cd, respectively, as observed through AFM micrographs. Notably, the grains appear columnar in shape, exhibiting an average particle size ranging (P_{av}) from 78.6 nm for undoped CuO to 42.1 nm for 4% Cd doping. Additionally, there is a discernible trend in surface roughness, which decreases from 6.82 nm to 3.23 nm, while the root mean square (RMS) roughness varies from 8.29 to 2.80 nm across the samples. The data presented in Table 2 indicate that the film surfaces are remarkably smooth [33]. Furthermore, the micrographs illustrate that pure and doped CuO films are spherical nanoparticles with a uniform distribution, indicating excellent crystalline quality. The high particle density per unit area and narrow size distribution further underscore the quality of the films. The observed reduction in grain size with increasing Cu loading can be attributed to the difference in ionic radii between Cu^{2+} and Cd^{2+}. This phenomenon has been documented in previous studies [34], corroborating the findings.

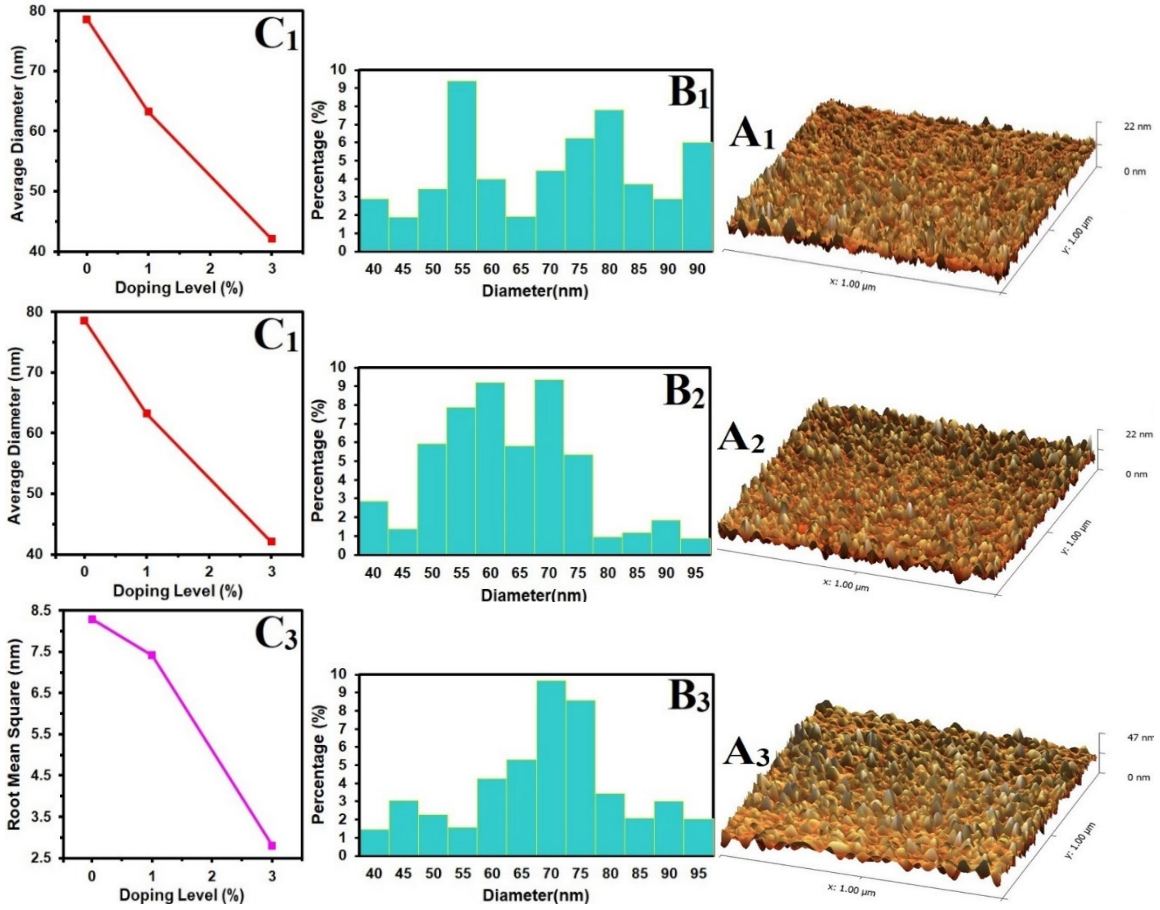

Fig. 3. AFM informations of the films.

Table 2. AFM data of the intended films.

Samples	P_{av} Nm	R_a (nm)	RMS (nm)
Undoped CuO	78.6	6.82	8.29
CuO: 1% Cd	63.2	3.87	7.41
CuO: 3% Cd	42.1	3.23	2.80

Surface morphology analysis of the prepared films, encompassing Undoped CuO and CuO: Cadmium films, was performed using scanning electron microscopy (SEM), as illustrated in Fig. 4. Examination of the SEM patterns revealed discernible trends. With an increase in the Cadmium content in CuO, there was an evident augmentation in the number of aggregations within the film, resulting in a more uniform structure. Clusters either aggregated, leading to voids, or grew atop a denser film. Consequently, this created a more porous structure in the 0% to 3% Cadmium-doped CuO films [35, 36]. This occurrence could be ascribed to alterations in the nucleation and growth behavior of the material induced by Cadmium ions.

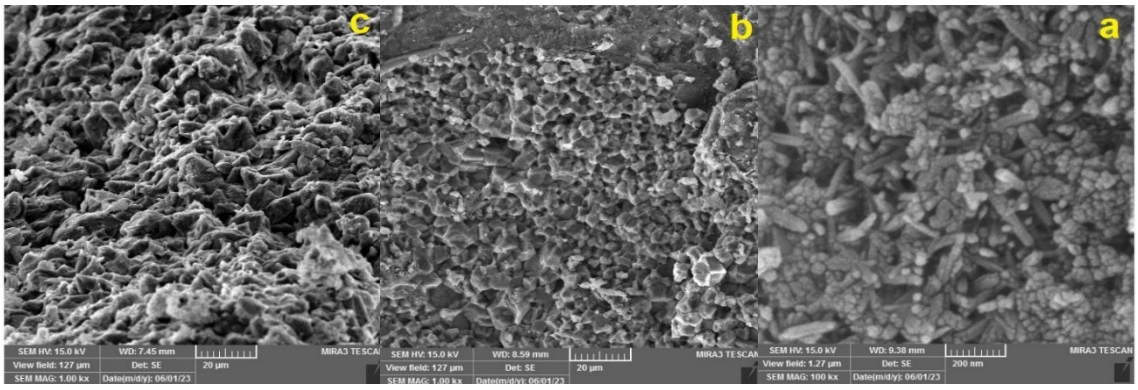

Fig. 4. SEM of the deposit film.s

The absorbance (A) was calculated using the following [37]:

$$A = 2 - \log 10\ (\%\ T) \tag{4}$$

where T is the transmittance. Fig. 5 show the absorption spectrum of the grown films films across the 300-900 nm wavelength range. Notably, in the visible region, there is a noticeable decrease in absorbance with increasing wavelength, while absorbance values rise with higher cadmium doping levels. This observation underscores the high absorbance of the manufactured films within the visible spectrum, making them well-suited for various applications [38, 39]. This discovery aligns with previous studies that also emphasized the films' substantial absorbance in the visible range, underscoring their versatility across diverse applications [40]. Moving to Fig. 6, it presents T spectra of both doped and undoped CuO films. The films exhibit optical transmittance exceeding 77%. However, cadmium doping reduces the transmission of CuO film, a crucial aspect of its potential use as window layers in solar cells. This decline in transmission could be attributed to increased photon scattering resulting from crystal defects, which may be associated with the microstructural characteristics of the produced films [41, 42].

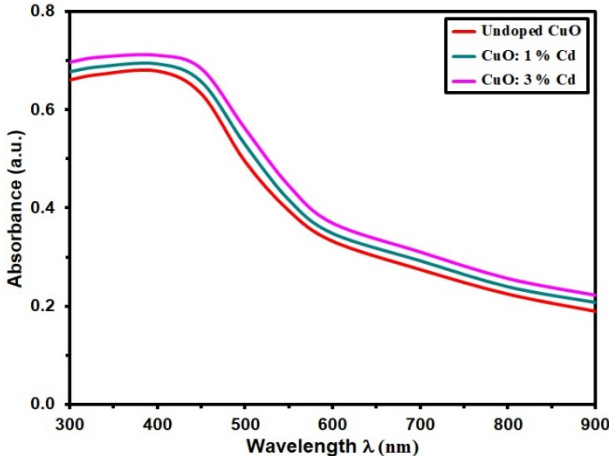

Fig. 5. Absorbance with wavelength of the grown films.

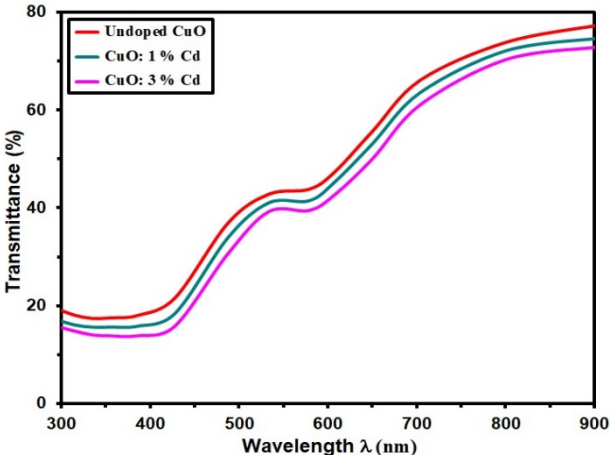

Fig. 6. Transmittance with wavelength of the grown films.

The absorption coefficient (α) is calculated using Eq. (5) [43]:

$$\alpha = \ln (1/T)/d \tag{5}$$

Here, d represents the film thickness. Fig. 7 displays α of CuO and Cd-doped CuO thin films deposited. High values of the absorption coefficient ($\alpha > 10^4$) indicate a high probability of a direct transition [44, 45]. The absorption coefficient depends on photon energy (hν) within the spectral region of 1-4 eV, with α increasing as photon energy rises. Notably, it has been observed that the absorption coefficient (α) increases with higher cadmium content [46].

The band gap energy (Eg) was determined using Eq. (6) [47]:

$$(\alpha h\nu) = A\left(h\nu - E_g\right)^{\frac{1}{2}} \tag{6}$$

where 'A' represents a constant, 'ν' denotes the frequency of incident radiation, and 'h' stands for Planck's constant. The resulting graph, depicted in Fig. (insert Fig. number), illustrates the relationship between α and hν. From this graph, the energy gap values for undoped CuO and 3% cadmium-doped CuO films were approximately 2.28 eV and 2.14 eV, respectively. These values were determined by extrapolating the linear portion of the curve to $(h\nu)^2 = 0$. Notably, the graph demonstrates a decrease in E_g value as Cd content rises. These observations align with findings reported by other researchers [48].

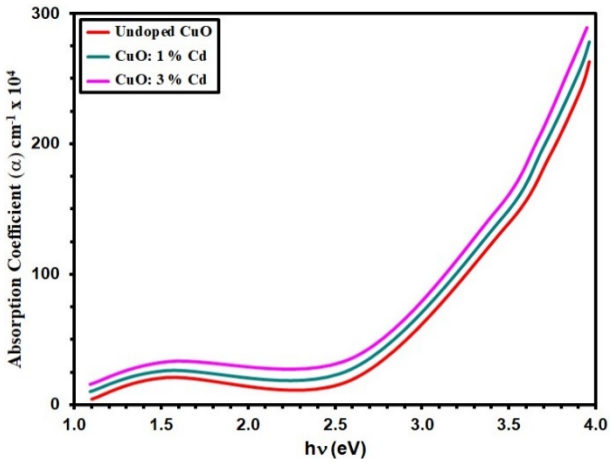

Fig. 7. α Vs hν of the prepared films.

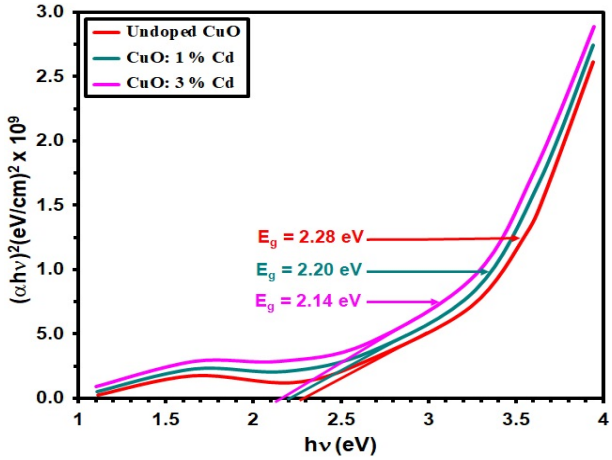

Fig. 8. $(\alpha h\nu)^2$ versus hν of the CuO with various Cd content.

The extinction coefficient (k) of undoped CuO and CuO: Cd thin films was calculated from the following expressions [49]:

$$k = \frac{\alpha\lambda}{4\pi} \tag{7}$$

The relationship between k and λ, as depicted in Fig. (9), was attributed to the increase in cadmium content in the film, as indicated in reference [50]]. k decreases as the doping ratio of cadmium increases. Additionally, k diminishes with the increase in wavelength. This phenomenon can be explained by the interaction between cadmium atoms and incident light, where higher cadmium content leads to more efficient absorption or scattering of light, resulting in a lower extinction coefficient. Additionally, the decrease in the extinction coefficient with increasing wavelength can be attributed to the wavelength-dependent optical properties of the material [51]. As the wavelength increases, the material may exhibit different absorption or scattering behavior, reducing the extinction coefficient.

The refractive indices (n) of CuO and CuO without doping Calculations of Cd thin films are made using the following formulas. [52]:

$$n = \left(\frac{1+R}{1-R}\right) + \sqrt{\frac{4R}{(1-R)^2} - k^2} \tag{8}$$

where (R) is the reflectivity, Fig. 10 illustrates the variation of n versus λ. It is evident that the n decreases with increasing cadmium doping concentration, a trend that can be attributed to the slower formation of crystals resulting from higher cadmium doping levels [48].

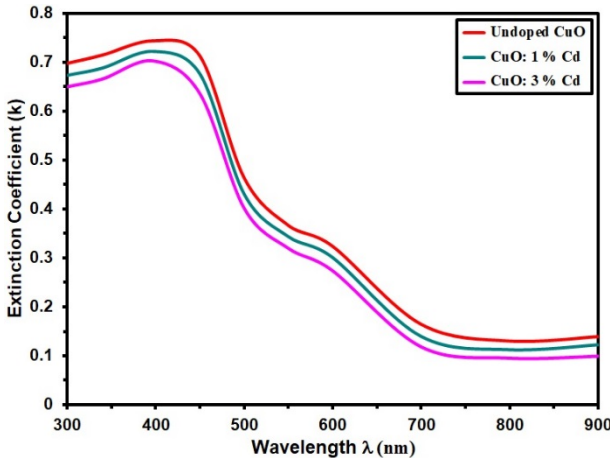

Fig. 9: k of the grown films.

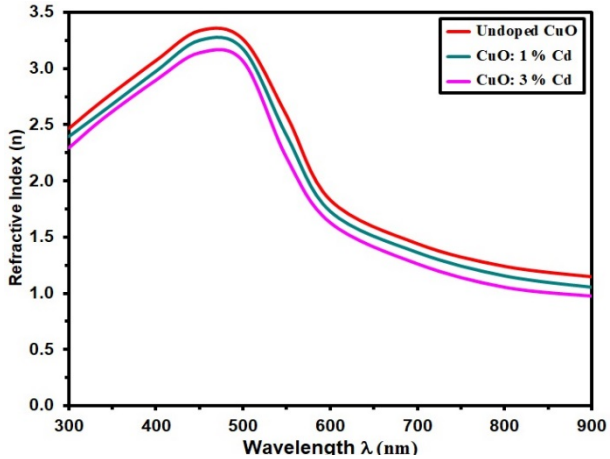

Fig. 10. n of grown films.

The gas sensor described utilizes a composite of porous silicon and a thin film of copper oxide (CuO) on glass to detect hydrogen (H_2) gas at a concentration of 375 parts per million (ppm) and an operational temperature of 50°C. The relationship between resistance and time for various compositions of the CuO thin film (Undoped, CuO: 1% Cd, and CuO: 3% Cd) at this concentration and temperature is depicted in Fig. 11. Upon contact with the sensor's surface, H_2 molecules trigger an oxidation process. This process involves the release of specific $O2^+$ ions from the surface, which subsequently release bonded electrons. These electrons then migrate back to the conduction band, resulting in an increase in resistance and the establishment of an enhanced potential barrier. The cadmium (Cd) doping level in the CuO film significantly influences the sensor's performance [53]. Notably, the CuO film doped with 4% Cd displayed the highest resistance among the tested compositions, suggesting its potential for heightened sensitivity in detecting H_2 gas.

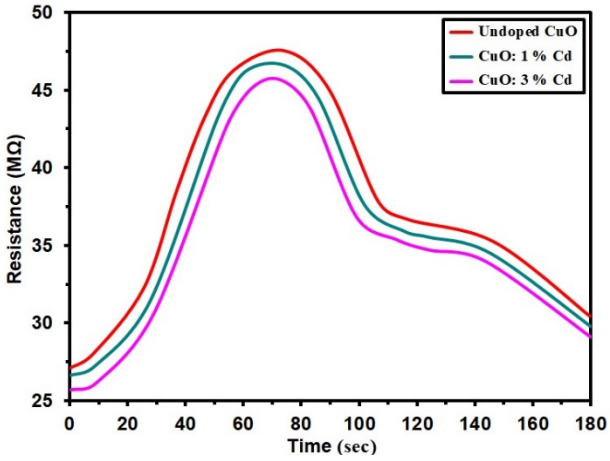

Fig. 11. depicts resistance over operating time for both Undoped and CuO: Cd films with various dopant concentrations.

The sensor's detection sensitivity, or response, can be calculated as [54]:

$$Sensitivity = \frac{\Delta R}{R_g} = \left|\frac{R_g - R_a}{R_g}\right| \times 100\ \% \tag{8}$$

Fig. (12) sensitivity plots depict how different doping levels (Undoped, CuO: 1% Cd, and CuO: 3% Cd) influence H_2 gas exposure. Sensitivity decreases with increased cadmium doping due to charge carrier recombination. Across various doping levels, sensitivity decreases from 32.1 % to 10.5 % at 125 ppm, 33.4 % to 11.6 % at 250 ppm, and 35.1 % to 13.4 at 375 ppm. This suggests that higher levels of Cadmium doping lead to reduced sensor responsiveness to hydrogen (H_2) gas [55].

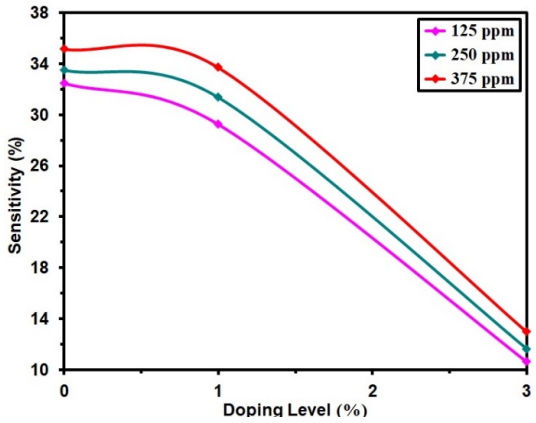

Fig. 12. The sensitivity of Undoped and CuO:Cd films with varying dopant concentrations.

4. Conclusion

Researchers studied CuO films prepared using the Sol-Gel technique, comparing undoped CuO films with those doped with Cadmium (CuO: Cd). XRD analysis revealed that all films were polycrystalline CuO. Upon doping with 4% Cadmium, the grain size of undoped CuO increased to 18.72 nm. Interestingly, as the Cadmium content increased, dislocation density and strain values decreased across all samples. Moreover, higher Cadmium concentrations led to notable reductions

in surface morphological features and nanostructural characteristics, including cluster grain size and porosity, in CuO films. SEM analysis showed Cadmium increased aggregation in CuO, yielding uniform structure. On 3%, clusters caused voids or porous structures due to Cd-induced growth changes. A UV-VIS spectrophotometer was utilized in the study.

The results showed that all optical parameters in the visible range of the electromagnetic spectrum decrease as the wavelength increases, except for transmittance, which increases. Additionally, it was observed that the energy gap value ranged from 2.28 eV to 2.14 eV, decreasing with higher levels of Cadmium doping. The gas sensor detects H_2 at 375 ppm using CuO film; cadmium doping improves sensitivity, with CuO: 3% showing the highest resistance. Sensitivity drops at 125 ppm (18.4% to 4.6%), 250 ppm (20.7% to 6.8%), and 375 ppm (25.9% to 8.2%).

Acknowledgements

The authors expressed their gratitude for the support provided by Mustansiriyah University (www. uomustansiriyah.edu.iq).

References

[1] M. T. S. Nair, L. Guerrero, O. L. Arenas, P. K. Nair, Appl. Surf. Sci., 150 (1) 143-151 (1999); https://doi.org/10.1016/S0169-4332(99)00239-1
[2] A. O. Ibhadon, P. Fitzpatrick, Heterogeneous Photocatalysis: Recent Advances and Applications, 12, 189-218 (2013); https://doi.org/10.3390/catal3010189
[3] G. Madec, P. Delecluse, M. Imbard, et C. Levy, Notes du Pôle Modélisation, Inst. Pierre Simon Laplace, 14 (4), (2014); https://doi.org/10.2478/adms-2014-0021
[4] L. Sun et al., Adv. Energy Mater., 9 (48). 1-11 (2019); https://doi.org/10.1002/aenm.201902839
[5] H. M. Jawad, A. M. Kadhim, F. A. Jasim, AIP Conference Proceedings, AIP Publishing 3097 (1), (2024); https://doi.org/10.1063/5.0209812
[6] H. M. Jawad, F. A. Jasim, AIP Conference Proceedings, AIP Publishing 3097 (1), (2024); https://doi.org/10.1063/5.0209811
[7] T. Oku, R. Motoyoshi, K. Fujimoto, T. Akiyama, B. Jeyadevan, J. Cuya, J. Phys. Chem. Solids, 72 (11), 1206-1211 (2011); https://doi.org/10.1016/j.jpcs.2011.06.014
[8] K. Y. Qader, E. H. Hadi, N. F. Habubi, S. S. Chiad, M. Jadan, J. S. Addasi, International Journal of Thin Films Science and Technology, 10 (1), 41-44 (2021); https://doi.org/ 10.18576/ijtfst/100107
[9] S. K. Muhammad, M. O. Dawood, N. Y. Ahmed, E. S. Hassan, N. F. Habubi, S. S. Chiad, Journal of Physics: Conference Series, 1660 (1), 012057 (2020); https://doi.org/ 10.1088/1742-6596/1660/1/012057
[10] R. P. Wijesundera, Semicond. Sci. Technol., 25 (2010); https://doi.org/10.1088/0268-1242/25/4/045015
[11].Y Li, J Liang, Z Tao and J Chen, Mater. Res. Bull, 43, 2380 (2008); https://doi.org/10.1002/aenm.200800795
[12] T. Koh, E. O'Hara, M.J. Gordon, J. Cryst. Growth, 363, 69 (2013); https://doi.org/10.1016/j.jcrysgro.2012.10.005
[13] M.R. Johan, M. S. M. Suas, N. L. Hawar, H. A. Ching, Int. J. Electrochem. Sci., 6, 6094 – 6104 (2011); https://doi.org/10.1016/S1452-3981(23)19665-9
[14] K. Mageshwari, D. Nataraj, T. Pal, R. Sathyamoorthy, J. Park, J. Alloys Compd. 625, 362 (2015); https://doi.org/10.1016/j.jallcom.2014.11.109
[15]. Kumar, A. S. K. Perumala, P. Thirunavukkarasu, Optoelec.Advan. Mater. –Rapid Commun. 4 (6),.831 – 833 (2010); https://doi.org/10.3390/coatings11111392
[16] K. Mageshwari, R. Sathyamoorthy, Mater. Sci. Semicond. Process., 16, 337 (2013);

https://doi.org/10.1016/j.mssp.2012.09.016
[17] M.H. Kabir, H. Ibrahim, M.M. Billah, AIP Conference Proceedings 2324, 030007 (2021); https://doi.org/10.1063/5.0037501
[18] M. Petrantoni, C. Rossi, L. Salvagnac, V. Con_ed_era, A. Est_eve, C. Tenailleau, P. Alphonse, Y.J. Chabal, J. Appl. Phys. 108 (2010); https://doi.org/10.1063/1.3498821
[19] H. Search, C. Journals, A. Contact, M. Iopscience, I. P. Address, Journal of Physics: Condensed Matter,, 18, 2417 (2006); https://doi.org/10.1088/0953-8984/18/8/007
[20] Pletea, M.; Bruckner, W.; Wendrock, H.; Kaltofen, R. J. Appl. Phys. 97, 054908 (2005); https://doi.org/10.1063/1.1858062
[21]. Samarasekara, P. "Characterization of low cost P-Cu2O/N-CuO junction" Physics, 2 (4), 3 (2010); https://doi.org/10.1016/j.solmat.2010.11.015
[22] F. A. Jasima , Z. S. A. Mosa, N. F. Habubi, Y. H. Kadhim, S. S. Chiad, Digest Journal of Nanomaterials and Biostructures, 18 (3), 1039–1049 (2023); https://doi.org/10.15251/DJNB.2023.183.1039
[23] A. A. Abdul Razaq, F. H. Jasim, S. S. Chiad F. A. Jasim, Z. S. A. Mosa , Y. H. Kadhimd, Journal of Ovonic Research, 20 (2), 131 – 141 (2024); https://doi.org/10.15251/JOR.2024.202.131
[24] S. K. Muhammad, N. D. M. Taqi, S. S. Chiad, K. H. Abass, N. F. Habubi, Journal of Green Engineering, 11(2), 1287-1299 (2021).
[25] E. S. Hassan, D. M. Khudhair, S. K. Muhammad, A. M. Jabbar, M.O. Dawood, N. F. Habubi, S. S. Chiad, Journal of Physics: Conference Series ,1660 (1) 1660 012066 (2020); https://doi.org/10.1088/1742-6596/1660/1/012066
[26] A. S. Alkelaby, K. H. Abass, T. H. Mubarak, N. F. , Habubi, S. S. Chiad, I. Al-Baidhany, Journal of Global Pharma Technology 11(4), 347-352 (2019).
[27] Khadayeir, A.A., Abass, K.H., Chiad, S.S., Mohammed, M.K., Habubi, N.F., Hameed, T.K., Al-Baidhany, I.A., Journal of Engineering and Applied Sciences, 13 (22), 9689-9692 (2018).
[28] Khadayeir, A. A., Hassan, E. S., Mubarak, T. H., Chiad, S.S., Habubi, N. F., Dawood, M.O., Al-Baidhany, I. A., Journal of Physics: Conference Series, 1294 (2) 022009(2019); https://doi.1088/1742-6596/1294/2/022009
[29] N. Y. Ahmed, B. A. Bader, M. Y. Slewa, N. F. Habubi, S. S. Chiad, NeuroQuantology, 18(6), 55-60 (2020); https://doi.org/10.1016/j.jlumin.2021.118221
[30] A. J. Ghazai, O. M. Abdulmunem, K. Y. Qader, S. S. Chiad, N. F. Habubi, AIP Conference Proceedings 2213 (1), 020101 (2020); https://doi.org/10.1063/5.0000158
[31] H. A. Hussin, R. S. Al-Hasnawy, R. I. Jasim, N. F. Habubi, S. S. Chiad, Journal of Green Engineering, 10(9), 7018-7028 (2020); https://doi.org/10.1088/1742-6596/1999/1/012063
[32] S. S. Chiad, H. A. Noor, O. M. Abdulmunem, N. F. Habubi, M. Jadan, J. S. Addasi, Journal of Ovonic Research, 16 (1), 35-40 (2020). https://doi.org/10.15251/JOR.2020.161.35
[33] H. T. Salloom, E. H. Hadi, N. F. Habubi, S. S. Chiad, M. Jadan, J. S. Addasi, Digest Journal of Nanomaterials and Biostructures, 15 (4), 189-1195 (2020); https://doi.org/10.15251/DJNB.2020.154.1189
[34] J. Chen, F. Zhang, J. Wang, G. Zhang, B. Miao, X. Fan, D. Yan, P. Yan, Journal of Alloys and Compounds, 454 (2008) 268-273; https://doi.org/10.1016/j.jallcom.2006.12.032
[35] S. Kulkarni, Y. Navale, S. Navale, F. Stadler, N. Ramgir, V. Patil, Sensors and Actuators B: Chemical, 288 (2019) 279-288; https://doi.org/10.1016/j.snb.2019.02.094
[36] M. D. Sakhil, Z. M. Shaban, K. S. Sharba, N. F. Habub, K. H. Abass, S. S. Chiad, A. S. Alkelaby, NeuroQuantology, 18 (5), 56-61 (2020); https://doi.org/10.14704/nq.2020.18.5.NQ20168
[37] R. Daira, S. Regaie, B. Boudjema, A. Harrouz, Algerian Journal of Renewable Energy and Sustainable development, 5 (1) (2023) ; https://doi.org/10.46657/ajresd.2023.5.1.10
[38] R. S Ali, N. A. H. Al Aaraji, E. H. Hadi, N. F. Habubi, S. S. Chiad, Journal of Nanostructuresthis link is disabled, 10(4), 810–816 (2020); https://doi: 10.22052/jns.2020.04.014
[39] R. S. Ali, M. K. Mohammed, A. A. Khadayeir, Z. M. Abood, N. F. Habubi and S. S. Chiad, Journal of Physics: Conference Series, 1664 (1), 012016 (2020); https://doi:10.1088/1742-6596/1664/1/012016

[40] A. A. Khadayeir, R. I. Jasim, S. H. Jumaah, N. F, Habubi, S. S. Chiad, Journal of Physics: Conference Series,1664 (1) (2020); https://doi.org/10.1088/1742-6596/1664/1/012009
[41] S. S Chiad,, A. S. Alkelaby, K. S. Sharba,, Journal of Global Pharma Technology, 11 (7), 662-665, (2020); https://doi.org/10.1021/acscatal.1c01666
[42] Chiad, S.S., Noor, H.A., Abdulmunem, O.M., Habubi, N.F., Journal of Physics: Conference Series 1362(1), 012115 (2019); https://doi.org/10.1088/1742-6596/1362/1/012115
[43] A. S. Al Rawas, M. Y. Slewa, B. A. Bader, N. F. Habubi, S. S. Chiad, Journal of Green Engineering,10 (9), 7141-7153 (2020); https://doi.org/10.1021/acsami.1c00304
[44] R. S. Ali, H. S. Rasheed, N. F. Habubi, S.S. Chiad, Chalcogenide Letters,, 20 (1), 63–72 (2023; https://doi.org/10.15251/CL.2023.201.63
[45] A. Ghazai, K. Qader, N. F. Hbubi, S. S. Chiad, O. Abdulmunem, IOP Conference Series: Materials Science and Engineering, 870 (1), 012027 (2020); https://doi.org/ 10.1088/1757-899X/870/1/012027
[46] B. A. Bader, S. K. Muhammad, A. M. Jabbar, K. H. Abass, S. S. Chiad, N. F. Habubi, J. Nanostruct, 10(4): 744-750, (2020); https://doi.org/ 10.22052/JNS.2020.04.007
[47] O. M. Abdulmunem, A. M. Jabbar, S. K. Muhammad, M. O. Dawood, S. S. Chiad, N. F. Habubi, Journal of Physics: Conference Series,1660 (1), 012055 (2020); https://doi.org/ 10.1088/1742-6596/1660/1/012055
[48] C. Chimeno-Trinchet, A. Fernández-González, J. Á. García Calzón, M. E. Díaz-García, R. Badía Laíño, Sci. Technol. Adv. Mater., vol. 20, no 1, p. 657-672, 2019 ; https://doi.org/10.1080/14686996.2019.1621683
[49] E. H. Hadi, M. A. Abbsa, A. A. Khadayeir, Z. M. Abood, N. F. Habubi, and S.S. Chiad, Journal of Physics: Conference Series, 1664 (1), 012069 (2020); https://doi.org/ 10.1088/1742-6596/1664/1/012069
[50] K. Y. Qader, R. A. Ghazi, A. M. Jabbar, K. H. Abass, S. S. Chiad, Journal of Green Engineering, 10 (10), 7387-7398 (2020); https://doi.org/10.1016/j.jece.2020.104011
[51] R. I. Jasim, E. H. Hadi, S. S. Chiad, N. F. Habubi, M. Jadan, J. S. Addasi, Journal of Ovonic Research, 19 (2), 187 – 196 (2023)..
[52] F. H. Jasim, H. R. Shakir, S. S. Chiad,N. F. Habubi, Y. H. Kadhi,, Jadan, M., Digest Journal of Nanomaterials and Biostructures, 18(4), 1385–1393 (2023); https://doi.org/10.15251/DJNB.2023.184.1385
[53] H. T. Salloom, R. I. Jasim, N. F. Habubi, S. S. Chiad, M. Jadan, J. S. Addasi, Chinese Physics B, 30 (6), 068505 (2021); https://doi.org/10.1088/1674-1056/abd2a7
[54] A. A. Al-Ghamdi, M. Khedr, M.S. Ansari, P. Hasan, M.S. Abdel-Wahab, A. Farghali, Physica E: Low-dimensional Systems and Nanostructures, 81, 83-90(2016); https://doi.org/10.1016/j.physe.2016.03.004
[55] X. Zheng, C. Xu, Y. Tomokiyo, E. Tanaka, H. Yamada, Y. Soejima, Physical Review Letters, 85, 5170 (2000); https://doi.org/10.1103/PhysRevLett.85.5170